Karst and urban flood-induced solid discharges in Mediterranean coastal rivers: The case study of Las River (SE France)

Christiane Dufresne, Bruno Arfib, Loic Ducros, Céline Duffa, Frank Giner, Vincent Rey

Karst and urban flood-induced solid discharges in Mediterranean coastal rivers: The case study of Las River (SE France)

Christiane Dufresne [a,b,c*], Bruno Arfib [d], Loïc Ducros [b,e], Céline Duffa [b], Frank Giner [b], and Vincent Rey [c]

[a.] Institut des sciences de la mer de Rimouski, Université du Québec à Rimouski, 310 allée des Ursulines, Rimouski QC, G5L 3A1, Canada

[b.] Institut de Radioprotection et de Sureté Nucléaire (IRSN), PSE-ENV, SRTE/LRTA, BP 3, 13115, Saint-Paul-lez-Durance, France

[c.] Université de Toulon, CNRS/INSU, IRD, Mediterranean Institute of Oceanography (MIO), UM 110, 83041 Toulon Cedex 09, France. / Aix Marseille Université, CNRS/INSU, IRD, Mediterranean Institute of Oceanography (MIO), OSU PYTHEAS, UM 110, 13288 Marseille, France

[d.] Aix Marseille Univ, CNRS, IRD, INRAE, Coll France, CEREGE, Aix-en-Provence, France. email : arfib@cerege.fr

[e.] Université de Nîmes, EA7352 CHROME, Laboratoire GIS, Parc scientifique et technique G. Besse, 150 rue Georges Besse, 30000 Nîmes, France

* corresponding author: christiane_dufresne@uqar.ca

Dufresne C., Arfib B., Ducros L., Duffa C., Giner F., Rey V. (2020) Karst and urban flood-induced solid discharges in Mediterranean coastal rivers: The case study of Las River (SE France). Journal of Hydrology. https://doi.org/10.1016/j.jhydrol.2020.125194

Abstract

Rivers solid discharge represents a substantial environmental issue, especially for the coastal marine environment. Unlike continental climate rivers, Mediterranean rivers show large discharge variability linked to rainfall, runoff and groundwater discharge, and can be temporary dry. Solid yields are difficult to predict due to variable source of floodwater. This paper assesses the suspended solid discharge of the Las River (SE France), a small stream in karst and urban environments, and its proportion due to flood events. Floods characteristics are analyzed to explore the variability of the solid yield and the influence of urban runoff and karst springs discharge, based on *in situ* data. The 35 floods events monitored during a 17 months survey largely contributed to the annual yield, with a proportion of 47% of the total water, and 69% of the total solid yielded in 11% of the time. The total rainfall and the total water discharge, related to the water levels in karst springs, drive the total solid yield, mostly composed of mud (90%). Urban runoff induces higher suspended solid concentration than karst flood, but generated a lower total solid yield. Karst springs, by expanding the catchment area of the stream, largely contribute to the total volume of water discharged to the sea and enhance the sand proportion due to their influence on the maximal water discharge. These results reveal the strong influence of the karst spring hydrodynamic functioning on the sediment yield to Mediterranean coastal environments. This study also highlights the efficiency of electric conductivity data to provide valuable insights about floodwater sources and sediment transport processes.

Keywords

Solid discharge; flood; runoff; urban stream; karst spring; Bay of Toulon

Highlights

- 69% of the total solid yield of the Las River occur during flood events
- Solid discharge is composed at 90% of mud
- Electrical conductivity efficiently distinguishes floodwater sources
- Karst flood events generate bigger solid yield and enhance sand proportions

1. Introduction

Coastal areas are very sensitive zones impacted by many anthropogenic and natural factors, where continental activities strongly influence the marine environment through rivers discharges. Sediments play an essential role in both aquatic and marine environments, as they influence nutrients dynamics but also contribute to contaminants transport. Although essential for bio-geochemical activities and responsible for some marine pollution, sediment fluxes in small rivers are poorly documented. Rivers solid discharge thereby represents a substantial environmental issue, especially for the coastal marine environment.

Unlike continental climate rivers, Mediterranean rivers show large discharge variability (Struglia *et al.* 2004) and solid yields are difficult to predict due to variable rainfall events and rivers temporary character (De Girolamo *et al.* 2015). A temporal average is barely significant because of the considerable discharge variation between the low flow and flood. Hydrologic sources include karst springs, rainfall events and urban runoff, while anthropogenic activities and uses of the watershed primarily impact rivers discharge (Cudennec *et al.* 2007). One may then be concerned by rivers solid discharge in coastal areas, especially in a Mediterranean highly touristic and marine-based economic region.

Quantification of sediment fluxes is all the more important in the Mediterranean region and arid and semi-arid areas, given that long dry periods and intense rainstorms cause unpredictable flash-flood of not only rivers but also temporary streams (Gaume *et al.* 2009). A single flash-flood event may alter the physical characteristics of the seawater column near the river's outlet for several days and its surface water for one month (Capello *et al.* 2016). Small rivers and ephemeral streams are generally un-gauged and little studied due to their limited economic impact, despite the need to understand their dynamics and processes (Tzoraki *et al.* 2007, Skoulikidis & Amaxidis 2009). Temporary rivers catchments yet represent 30% of the Mediterranean region (Moraetis *et al.* 2010), and their solid discharge might represent a significant proportion of total solid yield. For instance, Nicolau *et al.* (2012) estimated that flood discharge of the Eygoutier River (southern France, catchment ~ 70km^2) was responsible for more than 90% of the annual yield of suspended solids and particulate copper (Cu), zinc (Zn), cadmium (Cd) and lead (Pb). Large flood event in the Têt River (southern France, catchment ~1400 km^2) yielded about half of the annual total load within only a few days (Bourrin *et al.* 2008). Between 1980 and 1999, 78% of the total sediment was discharged from the Têt River to the Gulf of Lion (Western Mediterranean) within 50 days (Serrat *et al.* 2001). The solid discharge due to floods events in small coastal Mediterranean rivers is expected to contribute significantly to the total solid yield. Small rivers and urban streams have yet been understudied, but their contributions are commonly crucial for the local economy, flood risk assessment and management, and water supply (Skoulikidis *et al.* 2017). Their solid yields are also essential for the sedimentary budget of the entire marine system.

Triggered by rainfall, snowmelt or karst springs, flood events characterization usually relies on water discharge. Several other hydrological parameters and flood characteristics also provide insights on the solid discharge and the total yield. The event duration (López-Tarazón *et al.* 2010), the highest water discharge during the flood (Alexandrov *et al.* 2003, Zabaleta *et al.* 2007, López-Tarazón *et al.* 2010, López-Tarazón *et al.* 2012) and the total water volume (Serrat *et al.* 2001, Meybeck *et al.* 2003, López-Tarazón *et al.* 2010) are used in several studies to characterize flood events. Suspended solid characteristics, like the highest suspended solid concentration (SSC) (Meybeck *et al.* 2003, Zabaleta *et al.* 2007, Nadal-Romero *et al.* 2008), the total suspended sediment yield (Serrat 1999, Meybeck *et al.* 2003, Zabaleta *et al.* 2007) and the grain-size characteristics (Antonelli *et al.* 2008) shed light on the solid discharge variability. Finally, rainfall parameters such as the total rainfall, the rainfall intensity and the antecedent rainfall (Jungerius & ten Harkel 1994, Alexandrov *et al.* 2007, Zabaleta *et al.* 2007, Nadal-Romero *et al.* 2008, López-Tarazón *et al.* 2010) may also impact the solid discharge.

Because the electric conductivity (EC) acts as a tracer of the source of water and mixing processes, it has also been used to characterize flood events (e.g. Pilgrim *et al.* 1979, Valdes *et al.* 2006, Pellerin *et al.* 2008, Meriano *et al.* 2011). Rainwater, coming from evaporation and then condensation, has a very low EC (around 0 $\mu S \cdot cm^{-1}$). Following contact with surrounding soils, runoff may increase stream conductivity (Robson *et al.* 1993). Karst springs also show specific EC that may act as a signature and lead to identify hydrological processes, provided that the water EC is sufficiently distinct to distinguish the different contributions to the discharge. The flood event characteristics might thus be linked to the water sources (runoff or karst) with EC data (i.e. Robson *et al.* 1992, Valdes *et al.* 2006, Perrin & Tournoud 2009).

In this study, we focus on the Las River, in southern France, a typical small karst and urban Mediterranean coastal river. Carbonate rocks occupy 21.6% of the European land surface (Chen *et al.* 2017), where they form the dominant coastal rock in the northern part of the Mediterranean Sea (Fleury *et al.* 2007a). Mostly forming karst aquifers, their recharge area is usually distinct from the watershed. By enlarging the total catchment area of a stream, karst aquifers often increase both the water discharge and the sediment reserve.

Karst aquifers also have a peculiar hydrodynamic functioning due to large and permeable conduits, related to the speleogenetic history of the carbonate rocks (Jouves *et al.* 2017). Groundwater flows through the karst network and converges to the springs that concentrate the water discharge in few outlets. Karst springs discharge is then highly variable and can lead to flash-flood (Gaume *et al.* 2009, Fleury *et al.* 2013).

This paper aims to assess the total solid yield of a small urban river to the Mediterranean Sea and to explore floods characteristics influencing its solid discharge. Not only we estimate the annual solid yield, but we also analyze hydrological data from 35 events to focus on floods characteristics and to assess the solid discharge variability. More specifically, our goals are 1) to estimate the annual solid yield and its proportion due to flood events; 2) to characterize different types of flood events with EC, and 3) to identify environmental parameters that influence floods and their solid discharge.

2. The case study of the Las River

Located in the south of France, on the Mediterranean coast (Fig. 1), the Las River is a small urban stream (8 km long) flowing through the city of Toulon (170 000 inhabitants, population density of 4000 inhabitants per km^2). It is the only river flowing into the Little Bay, the western sub-basins of the Bay of Toulon that shelters the military and civilian harbors. The Bay of Toulon is submitted to intense anthropogenic pressure (French Navy, commercial traffic, industry, raw sewage) where many economic activities (nautical and touristic activities, mussel and fish farming) take place. Previous studies have shown the high contamination of the bottom sediment of the Bay of Toulon (Tessier *et al.* 2011, Dang *et al.* 2014, Dang *et al.* 2015), demonstrating the need to understand the hydro-sedimentary processes and sources of sediment supply. The suspended solid yield to the Bay remains the missing link for such processes and represents a gap to fulfill to further understand, explain and conserve its coastal system. Because of its high population density and its strong influence on economic activities, the Las River is a proper case study location, with typical Mediterranean climate conditions, various uses of the watershed, several hydrologic sources and a crucial necessity for water supply.

2.1. Catchment

The area has a typical Mediterranean climate with mild winters and dry summers. The 30-year interannual rainfall is 640 mm with less than 55 rainy days per year on average (Toulon weather station, Météo-France, 2017).

The Las River catchment area is dual, composed of a groundwater recharge area supplying the karst springs and a surface watershed around its valley. Jurassic and Cretaceous carbonate rocks (mainly limestone and dolostone) form the geological environment and an extensive karst system covers the surrounding area. Karst features, including sinkholes, dolines, polje, karren and caves, favor the concentration of water infiltration and create a very dynamic aquifer, with fast and significant variation of flow rate (Baudement *et al.* 2017). This limestone plateau (Siou-Blanc) is a large catchment area (~70 km^2) for groundwater recharge of the Dardennes aquifer, mainly discharging at the Dardennes springs (Baudement *et al.* 2017). Karst springs provide the seasonal varying low-flow water discharge in the Las River and cause karst floods during rainfall events. Diversified land-use characterize the watershed, ranging from natural and former agricultural land upstream, to urban areas close to the Las valley and the Mediterranean Sea. A large part of the rainfall infiltrates over the karst natural or formal agricultural land, and surface runoff is almost nil on the carbonate hills. Runoff is then roughly limited to the downstream urban area, covering an area of 14 km^2, and the urban drainage network transports water that converges from hills to the Las valley.

2.2. Karst springs and river morphology

Two main karst springs are referenced (Fig. 1): the Dardennes springs at the upstream location of the Las valley (8 km from the sea) and the Saint-Antoine spring (3.6 km from the sea). The latter's discharge ranges from 0.01 $m^3 \cdot s^{-1}$ to 4 $m^3 \cdot s^{-1}$ (Arfib, unpublished data, 2019). Other springs exist with insignificant discharge (as the Baume de Dardennes spring) and may be negligible compared to the two previous zones.

The Dardennes springs are of significant importance for the city of Toulon since they provide drinking water for more than a century. Downstream the springs, a dam built in 1913 creates a reservoir which provides drinking water during the low flow period (maximum stored volume $1.1 \cdot 10^6$ m^3). The reservoir water level (H_{RES}) is controlled and monitored by the drinking water treatment plant and fluctuates from 123 m above sea level (m a.s.l.) in winter to 110 to 115 m a.s.l. in summer. Above 123 m the reservoir water overflows by a spillway to the downstream Las River. For management purpose (rarely occurring), the opening of flush-valves of the dam regulates the reservoir water level. Dardennes karst springs generate

a near-bottom current which prevents the settling of sediments in the reservoir and favours a solid discharge to the Las River through the water treatment plant.

The natural discharge of the Dardennes springs is close to 0.1 $m^3 \cdot s^{-1}$ during the low-flow period in summer, withdrawn for the freshwater supply. During floods, karst discharge can exceed 20 $m^3 \cdot s^{-1}$ and is closely linked to the rainfall amount over the recharge area (Baudement *et al.* 2017). A vauclusian overflow spring, called "Ragas" spring and located 500 m upstream the reservoir, discharges groundwater during flood events when a threshold level at 149 m a.s.l. is exceeded. The Ragas karst conduit acts as a natural piezometer in the karst network, and its level (H_{Ragas}) reflects the periods of a possible high contribution of karst groundwater to the Las River.

The Las river has a straight channel, constrained by the hill slopes surrounding the valley. Its width is almost constant, 10 m large. The water height ranges from few centimeters at low-flow to two meters in flood, and its bed is natural with coarse pebble and gravel. The gradient is high, 14 per mil in average between the Dardennes springs and Saint-Antoine spring. The downstream 3 km have been channelized, the first 2km with concrete.

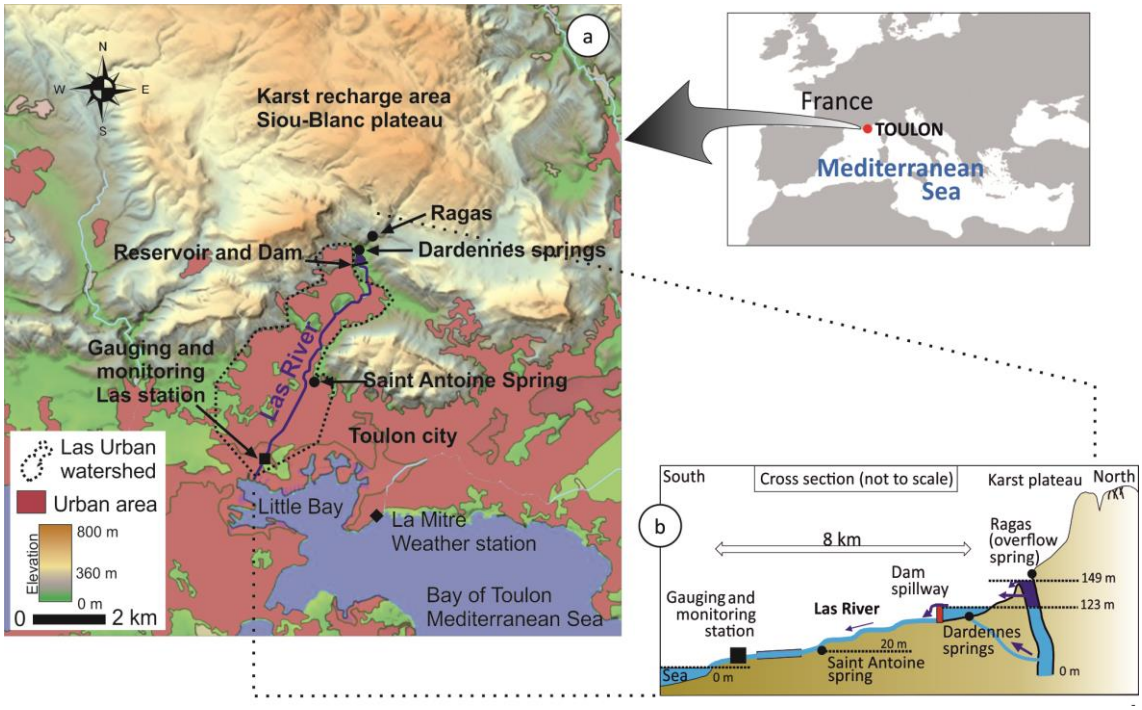

Fig. 1. (a) Location of the Las River catchment with karst springs (dots), reservoir and dam, monitoring station (square) and *La Mitre* Météo-France weather station (diamond); (b) schematic cross-section of the Las River

3. Methodology

3.1. Instrumental setup

We assessed the solid discharge with climatic datasets and hydrological observations recorded both at the source and the mouth of the Las River. The location of the monitoring station near the river's mouth was selected accordingly to accessibility and technical constraints (square in Fig. 1), as far downstream as possible. The vast majority of tributaries (such as possible underground springs, stormwater outlet, urban runoff) were thus taken into account. A 2 meters high waterfall located 100m upstream the monitoring station favors a complete mixing of the water column and homogeneous SSC. We assumed that recorded data is representative of the entire vertical cross-section and consequently, of the solid discharge to the sea. A multi-parameter probe and a sediment trap were deployed continuously for 17 months, from October 2012 to March 2014. The multi-parameter probe recorded temperature, pressure, turbidity and electric conductivity data every 5 minutes. The sediment sampler, fully described by Phillips *et al.* (2000), is designed to trap suspended matter that flows in the stream by slowing down the ambient flow, which induces sedimentation by settling. Its efficiency in trapping a representative time-integrated sample of the suspended solid discharge has been showed (Phillips *et al.* 2000, Russell *et al.* 2000) and verified for the Las River (see Appendix A). Sediment trap samplings were processed with a laser diffraction particle size

analyzer that provides size distribution in volume with a sizing range from 0.04 to 2000 µm. 155 water samples were also collected punctually at the same station to estimate the SSC and to convert the recorded turbidity data into concentration. Upstream, near the river's sources, CTD probes were deployed to characterized the three karst springs (Ragas, Dardennes, Saint Antoine) at a 15 minutes time-step.

3.2. Rainfall and water discharge

The French meteorological network Météo-France provided the rainfall data, recorded at *La Mitre* weather station (diamond in Fig. 1). This station is located 4 km from our monitoring station, close to the sea, in the same climatic environment. Using only one rain-gauge, we assume that the rainfall is homogeneous over Toulon city and the Las catchment, and so this station is representative of the rainfall over the urban watershed of the Las River. For further discussion about the rainfall over the karst recharge area, out of the scope of this paper, several rain-gauges must be used to capture the rainfall heterogeneity, as done in Baudement *et al.* (2017).

The Las River flow was estimated with a rating curve, linked to the water height at the monitoring station (square in Fig. 1). The rating curve was established with 41 discharge measurements carried out with the dilution method by injection of a fluorescent dye (Schnegg *et al.* 2011, Lamarque 2014) between August 2013 and January 2014 (during the monitoring period).

3.3. Data analysis

3.3.1. Relationship turbidity/suspended solid concentration

The SSC is deduced from turbidity data, which indicates the water opacity. Establishing a single relationship between the turbidity data and the SSC for each monitoring station is essential, since the suspended matter characteristics (e.g. size, mineralogy) (Lenzi & Marchi 2000) influence the turbidity response and might change depending on the location. We established a specific NTU/SSC relationship for our monitoring station from the recorded turbidity data and the SCC from water samplings filtrations (see appendix B).

3.3.2. Selection of flood events

We selected flood events based on the water discharge by using the Filtered Peaks Over Threshold (FPOT) method (Claps & Laio 2003). All the local maxima of the time series were first selected and filtered (step 1) to obtain a sequence of discharge rises relative to the base level preceding the event. A second filter was applied to retain only the largest peaks (step 2) and to ignore the smallest events and false peaks induced by the noise component of the signal. A threshold of 1 $m^3 \cdot s^{-1}$ was defined graphically to be higher than the daily noisy discharge variations and to keep a maximum of relevant flood events. A lower value would have included a small number of additional short events, with a minor impact on the volume of water and the total solid discharge. However, this threshold is a key factor for flood frequency analysis (Lang *et al.* 1999, Bezak *et al.* 2014), and the time-series should be reprocessed for further analysis. When several peaks succeed one another within less than 12 hours, successive floods peaks were merged in one single flood event (Fig. 2).

3.3.3. Characterizing flood events

Events-based characteristics regarding hydrological features, the suspended solid discharge and rainfall for each flood events are summarized in Table 1, with their abbreviation and units. The duration of selected events is based on the start and the end times. The start time is taken when the water discharge started to increase. The end of the event is, by contrast, not trivial and depends on the shape of the recession limb of the hydrograph. Flood recession hydrographs have been commonly described by a rapid falling limb followed by one or a series of exponential recessions, which are characterized by one or several slopes depending on the baseflow variations (Chow 2010). We adopted a method to include the rapid falling limb and the first baseflow recession time. The flood event thus lasts until the inflection point at the end of the first baseflow recession slope (Fig. 2). This method has the advantage to be easily applied and integrates the flood peak and the first part of the delayed recession flow while excluding the effects of a long tailing discharge recession.

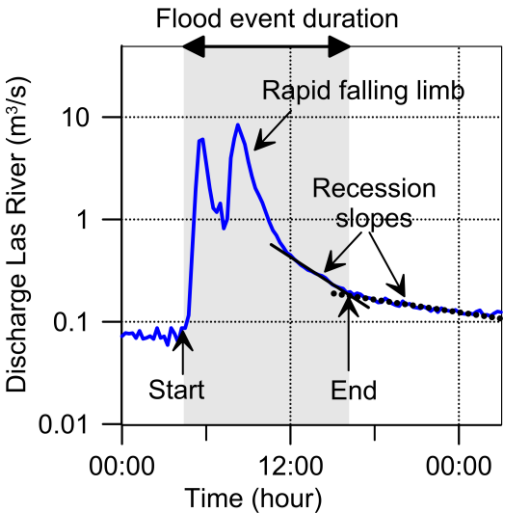

Fig. 2 Method to identify the start and end time of the flood events. Example for the event of the 8th of September 2013, with two peaks and 2 main recession slopes after a rapid falling limb of the hydrograph.

Rainfall characterizes the events with the total rainfall during the flood event and rainfall intensities (6min and 1h). Because rainfalls frequently occur before the increase of the water discharge (and consequently before the beginning of the selected flood event), previous rainfalls are also taken into account (antecedent rainfalls parameters).

Relationships among all of these parameters are investigated with a Pearson correlation matrix, an appropriate analysis to identify factors that might control the measured hydrological and sedimentary responses (Zabaleta *et al.* 2007, Nadal-Romero *et al.* 2008).

Table 1: Names, abbreviation and units for the event-based parameters used to describe the selected 35 flood events

Parameters	**Abbreviation**	**Unit**
Time		
Event duration	*Duration*	h
Liquid discharge		
Maximum water discharge	Q_{MAX}	$m^3 \cdot s^{-1}$
Total water discharge (Volume)	W_{TOT}	m^3
Solid discharge		
Maximum suspended solid concentration	SSC_{MAX}	$mg \cdot L^{-1}$
Average suspended solid concentration	SSC_{AVE}	$mg \cdot L^{-1}$
Total suspended solid discharged (mass)	Sol_{TOT}	kg
Electric conductivity (with 25°C reference temperature)		
Minimum electric conductivity	EC_{MIN}	$mS \cdot cm^{-1}$
Average electric conductivity	EC_{AVE}	$mS \cdot cm^{-1}$
Maximum electric conductivity	EC_{MAX}	$mS \cdot cm^{-1}$
Rainfall during the flood event		
Total rainfall	*TotRain*	mm
Maximum rain intensity in 6 minutes	*MaxInt6min*	$mm \cdot 6min^{-1}$
Maximum rain intensity in 1 hour	*MaxInt1h*	$mm \cdot h^{-1}$
Rainfall before the flood event		
Antecedent rainfall 1 day (24h before the flood event)	*AnteRain1*	mm
Antecedent rainfall 7 days	*AnteRain7*	mm
Antecedent rainfall 14 days	*AnteRain14*	mm
Water levels		
Dardennes Reservoir minimum water level in the hour preceding the beginning of the flood	H_{RES}	m
Ragas karst spring maximal water level	H_{RAGAS}	m

3.3.4. Sources of water

The discharge water of the Las River originates from different sources, mixed in various proportions. We distinguish the two karst groundwater discharge zones (Dardennes springs and Saint-Antoine spring) and the urban runoff of the city of Toulon with the water levels in the karst springs and the EC at the monitoring station. Main karst flood events from Dardennes springs are characterized by a disconnection between the water levels from the Ragas spring (H_{Ragas}) and the Dardennes reservoir (H_{RES}), with a peak water level up to the Ragas cave threshold (149 m a.s.l). The 123 m a.s.l. threshold of the Dardennes reservoir controls the discharge of karst groundwater to the Las river. Rocks of the aquifer and the residence time of groundwater induce different EC, representative of the Total Dissolved Solids in the water column. EC values act as a signature for different sources of water, identified with CTD measurements in karst springs. EC of the runoff water in Toulon has been measured during rainfall event in road gutter draining stormwater.

We defined three categories of floodwater sources in the river. (i) An increasing water discharge combined with runoff EC values and an unchanged karst level creates an urban runoff (UR) flood only due to rainfall. (ii) The groundwater from Dardennes karst springs fills the reservoir and only supply the river when overflowing the dam spillway (H_{RES} > 123 m a.s.l.). This karst overflow (KO) creates a sudden rise of the river discharge combined with characteristic EC values of the Dardennes springs. (iii) To prevent this massive water discharge, managers occasionally open the dam's valves, usually during and after a karst flood. This management (M) maintains H_{RES} under 123 m a.s.l. and sustains the discharge for a few days (slow recession). All combinations of sources of water are possible (UR and/or KO and/or M).

4. Results

4.1. Las River hydrological response

Data is available for 462 days over 522 days of *in-situ* monitoring and shows the highly variable hydrological response of the Las River (Fig. 3). The water discharge (Q) shows significant variations, ranging from 0.01 to 37.5 $m^3 \cdot s^{-1}$ (Fig. 3b). The mean discharge (Q_{AVE}) is about 1.66 $m^3 \cdot s^{-1}$, and the total volume of water discharged (W_{TOT}) (in 462 days) is $74 \cdot 10^6$ m^3. Q was higher than Q_{AVE} for 101 days, which yield a water volume of $59 \cdot 10^6$ m^3. Consequently, 80% of the total water volume is discharged to the sea in less than 22% of the time.

Each of the water sources of the Las catchment has a specific EC signature and their contributions induce fluctuations of EC within the river (Fig. 3c). The EC of the Dardennes springs ranges from 440-520 $\mu S \cdot cm^{-1}$ (mean=481 $\mu S \cdot cm^{-1}$, st.d.=23 $\mu S \cdot cm^{-1}$, n = 49421), and could reach 400 $\mu S \cdot cm^{-1}$ for heavy rainfall. The Saint-Antoine spring has an EC signature of 550-650 $\mu S \cdot cm^{-1}$ (mean=602 $\mu S \cdot cm^{-1}$, st.d.=34 $\mu S \cdot cm^{-1}$, n = 50113). Runoff low EC value is highly different from the karst groundwater and is within the same range of other urbanized area (Meriano *et al.* 2011), with a mean around 80 $\mu S \cdot cm^{-1}$ (st.d. 27 $\mu S \cdot cm^{-1}$, n = 37).

During low flow, EC in the river is close to 600 $\mu S \cdot cm^{-1}$, *i.e.* with the main contribution from the Saint-Antoine Spring (downstream from the dam). Floods globally induce a decrease of EC with fast drop to less than 100 $\mu S \cdot cm^{-1}$ due to the input of rainstorm and intermediate values (450-500 $\mu S \cdot cm^{-1}$) from Dardennes springs (including the Ragas spring overflow). During the flow recession following a flood, EC increases from 450 to 600 $\mu S \cdot cm^{-1}$ with mixed water from Dardennes springs and Saint-Antoine spring.

The water level in Dardennes springs shows the seasonality of the hydrological response of the Las River. During the warm and dry season (June to October), rainfalls are scarce and the water level in the karst decreases. The water level in the reservoir remains below 123m and runoff largely contributes to the river's discharge, as depicted by low EC values in the river (e.g. September, October 2013). As the first autumn rainfalls refill the karst, the water levels in Dardennes springs and in the reservoir increase with little influence on Q. Contributions of Dardennes springs significantly increase once the water level in the reservoir reaches the dam spillway threshold (123m), or when flush-valves are opened.

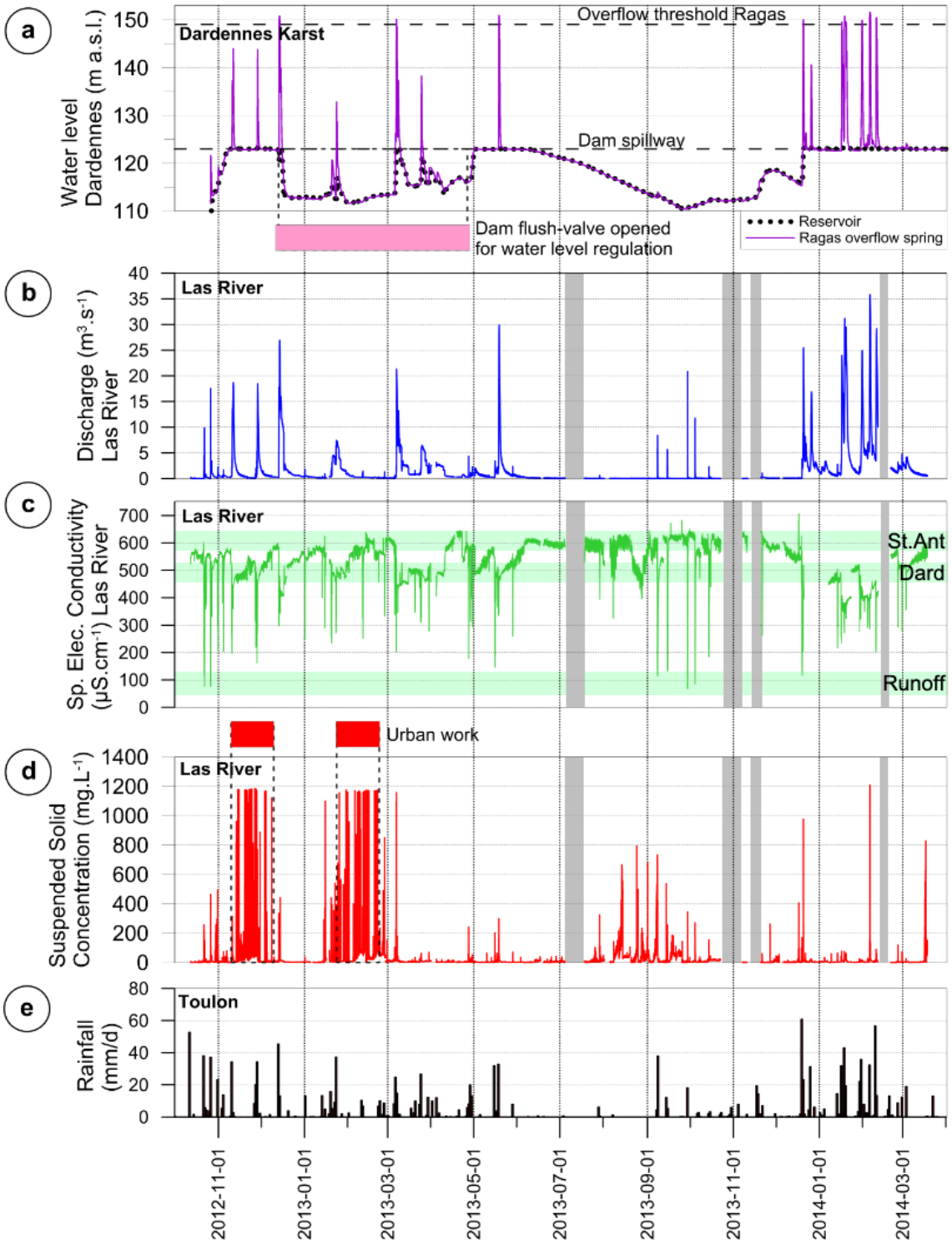

Fig. 3 (a) Water levels at Dardennes springs, (b) water discharge ($m^3 \cdot s^{-1}$) in the Las River, (c) Specific Electric Conductivity ($\mu S \cdot cm^{-1}$) at the monitoring station with the range of values for sources of water Saint-Antoine spring (St.Ant), Dardennes springs (Dard) and runoff in light green, (d) suspended solid concentration ($mg \cdot L^{-1}$), and (e) cumulated daily rainfall (mm). Gray vertical shadings show the measuring gaps.

4.2. Suspended solid discharge

4.2.1. Suspended solid concentration

In low-flow, the average SSC is 5 mg·L^{-1}, while during floods SSC reaches more than 1000 mg·L^{-1}. One may note that this value is out of the manufacturer range, up to 1000 NTU matching to 996 mg·L^{-1} (with Eq.B.1 in Appendix B). Values over this threshold might thus be misestimated. However, these very high SSC values mostly recorded in November 2012 and February 2013 were not due to flood events. Most of the largest SSC over this period were recorded in low flow and are most likely due to road works (Fig. 3d). Other high SSC values might be caused by unauthorized discharge or obstruction of the turbidity probe by floating wastes at the end of summer and autumn 2013. Despite the high SSC induced by those events, the associated solid yield is low regarding *Q* and the total solid yield to the Bay. The SSC time-series from November 2013 to March 2014 (end of available data) (Fig. 3d) shows a more natural evolution, with SSC peak related to rainfall events. Despite the apparent impact of the flood and water discharge on the suspended load, no clear relationship links *SSC* to *Q* (Fig. 4a), and the highest water discharges do not directly lead to the highest suspended loads.

The SSC is multiplied with *Q* at each time-step to deduce the solid flux. The solid flux increases during flood events and is usually comprised between 2 and 5 kg·s^{-1} with a maximum value of 14 kg·s^{-1}. The typical step-shape of the cumulative daily solid discharge plot (Fig. 4b) clearly shows the short main discharge periods and the decisive influence of flood events. About 1340·10^3 kg of suspended matters were brought to the sea during the recorded 17 months period, including two winters but only one summer. To assess the annual discharge, we calculated a 365-days moving average, which leads to an approximate annual yield of 707·10^3 kg ·y^{-1} (s.d. 108·10^3 kg). Approximately 1050·10^3 kg of suspended solid were yielded when Q was exceeding Q_{AVE}: 78% of the solid yield is carried in 22% of the time.

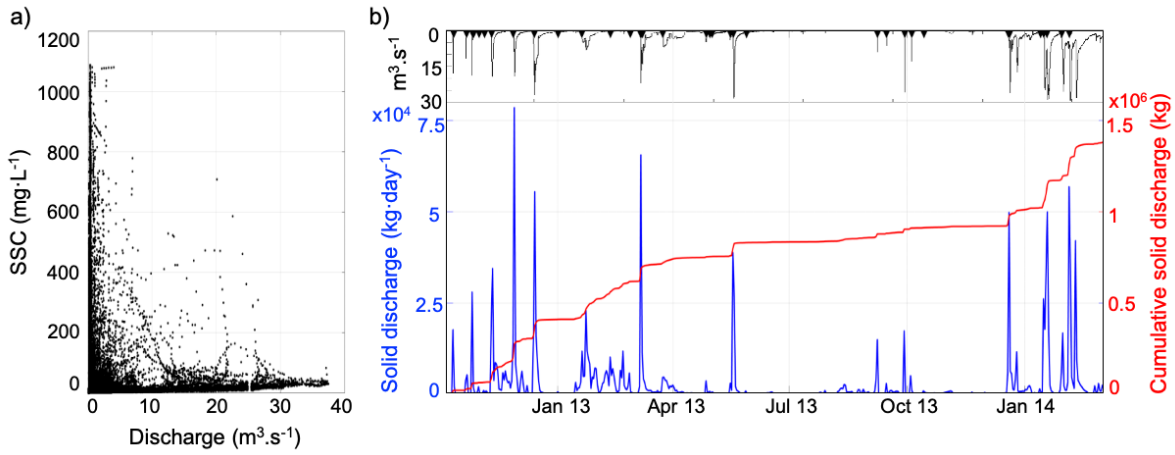

Fig. 4. a) Suspended sediment concentration (SSC, mg·L^{-1}) against discharge (Q, m^3·s^{-1}); b) Discharge (Q, m^3·s^{-1}) (black), Solid discharge (kg·day^{-1}) (blue) and cumulative solid yield (kg) (red) from October 2012 to March 2014. Black arrows mark selected flood events.

4.2.2. Grain-size characterization of the suspended solid discharge

Grain-size analyses were conducted on the 28 samples from the sediment trap to characterize the suspended matter of the Las River. Most loaded samples are from flood season, with a highest total dry mass in fall and spring. Fig. 5 shows the proportion of 5 grain-size classes (0.04–4 µm, 4–20 µm, 20–63 µm, 63–200 µm, 200-2000 µm) for the samples, with mud (D<63 µm, 3 classes) in blue shades and sand (D>63 µm, 2 classes) in red shades. Mud composes almost 90% of the total sediment yield (Table 2). Fine silt (4-20 µm) shows the biggest proportion, with 40.6% on average. The smallest clay particles (0.04-4 µm) compose a quarter of the sediments collected, but also show the greatest variability (s.d. 13.6). Some samples stand out with high sand proportions, as in March-April 2013, September-October 2013 and in December 2013, when sand composes almost 30% of the sediment samples (Fig. 5).

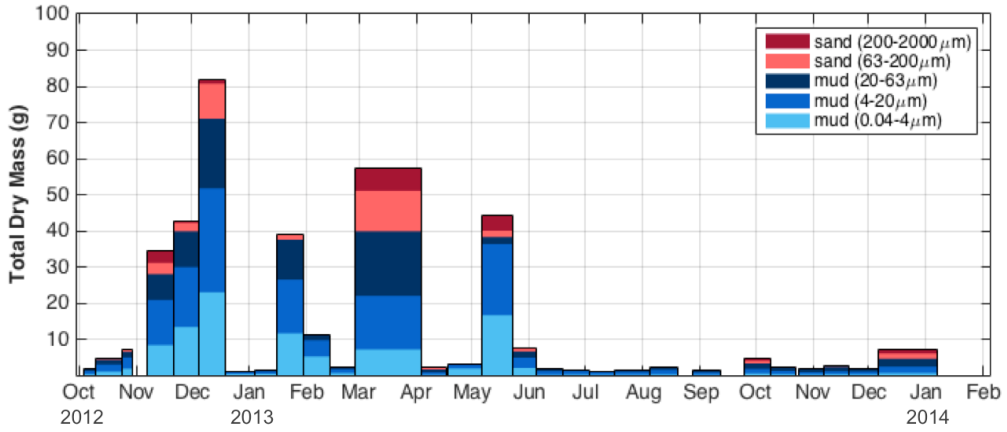

Fig. 5 Proportion of each grain-size class for the 28 sediment samples with mud in blue and sand in red. The width of bars is proportional to deployment duration.

Table 2. Mean proportion (%) and standard deviation of sediment samples for each grain-size class and gathered in mud (<63µm) and sand (>63µm) type.

	Sediment class (µm)	Proportion (%) [St. deviation]
Mud	0.04-4	24.6 [13.6]
	4-20	40.6 [6.8]
	20-63	24.5 [9.9]
Sand	63-200	6.9 [5.7]
	200-2000	3.3 [4.7]

4.3. Flood events characterization

Based on the methodology described in section 3, we selected 35 flood events (Table 3) which were characterized with parameters identified in Table 1 and sources of water as described in section 3.3.4. Selected floods events lasted between 2.3 h and 162.5 h (6.8 days) and are characterized by rainfalls ranging from 0 mm to 81.7 mm. Flood events yielded between $11.5 \cdot 10^3$ m^3 and $5.54 \cdot 10^6$ m^3 of water and between 408 kg and $105 \cdot 10^3$ kg of suspended solids, with SSC_{AVE} between 4 $mg \cdot L^{-1}$ to 408 $mg \cdot L^{-1}$. These events contributed to approximately 47% of the total water discharge and about 69% of the total solid yield. Summed up, these events durations represented 1188 h (~49.5 days), being 11% of the studied period. According to the hydrograph, karst water levels and EC, we identified 20 UR floods, 3 KO floods and 12 floods from mixed sources: 9 UR and KO, 2 UR and M, and 1 UR, KO and M.

We investigated the flood characteristics with a Pearson correlation matrix (Table 4) with regards to the solid yield. Very significant correlations (with an assumption of non-correlation p inferior to 0.01) are in bold and significant correlations (p<0.05) are underlined. The positive and very significant correlation between W_{TOT}, Q_{MAX} and Sol_{TOT} shows the influence of the water discharge on the solid discharge. Similarly, the positive and very significant correlations between Sol_{TOT} and both *TotRain* and H_{RAGAS} suggest that higher total rainfalls and higher water levels in the Ragas spring increase the solid discharge. The floods events characteristics and their impact on the solid discharge are further discussed in the following section.

Table 3: Flood events characteristics. UR: urban runoff; KO: karst overflow; M: dam opening management. Refer to Table 1 for abbreviations and units.

ID	Start time	Source of water	Duration (hour)	Q_{MAX} ($m^3 \cdot s^{-1}$)	W_{TOT} ($\cdot 10^3 m^3$)	SSC_{MAX} ($mg \cdot L^{-1}$)	SOL_{TOT} (kg)	SSC_{AVE} ($mg \cdot L^{-1}$)	EC_{MIN} ($mS \cdot cm^{-1}$)	EC_{AVE} ($mS \cdot cm^{-1}$)	EC_{MAX} ($mS \cdot cm^{-1}$)	TotRain (mm)	MaxInt6min ($mm \cdot 6min^{-1}$)	MaxInt1h ($mm \cdot 1h^{-1}$)	AnteRain1 ($mm \cdot 1d^{-1}$)	AnteRain7 ($mm \cdot 7d^{-1}$)	AnteRain14 ($mm \cdot 14d^{-1}$)	H_{RES} (m)	H_{RAGAS} (m)
1	2012-10-11 12:55	UR	14.6	17.77	130	251.8	19633	151.1	0.073	0.245	0.615	50.3	7.4	22.2	2.2	2.2	5.0	100.57	100.55
2	2012-10-21 17:15	UR	19.7	11.61	105	255.2	8967	85.6	0.075	0.337	0.587	2.2	0.4	0.6	3.2	4.8	57.5	102.15	104.18
3	2012-10-26 10:30	UR	5.5	18.81	89	424.7	23392	262.8	0.071	0.233	0.467	28.9	3.9	16.6	5.4	20.7	22.3	103.91	115.85
4	2012-10-27 3:15	UR	13.0	3.90	82	47.6	1325	16.1	0.329	0.476	0.507	3.8	2.4	1.2	37.2	52.5	54.1	110.16	115.20
5	2012-10-31 9:30	UR	13.0	2.57	47	212.3	1739	36.7	0.206	0.337	0.535	20.8	0.8	4.5	2.4	43.6	58.7	114.49	117.57
6	2012-11-04 16:30	UR	4.5	2.12	20	95.6	727	36.1	0.194	0.317	0.545	11.3	1.5	5.2	8.0	31.2	84.3	118.86	119.58
7	2012-11-10 9:15	UR + KO	88.5	19.25	2264	607.1	67531	29.8	0.197	0.443	0.507	35.3	3.1	6.5	2.4	21.5	44.7	123.02	143.96
8	2012-11-27 3:00	UR + KO	85.5	19.06	1758	1079.7	104808	59.6	0.156	0.437	0.525	62.8	2.2	6.2	2.4	2.4	2.6	122.96	143.78
9	2012-12-13 17:15	UR + KO + M	88.4	28.09	4350	334.6	98318	22.6	0.296	0.416	0.547	52.4	3.5	15.9	6.1	7.5	10.3	122.41	150.79
10	2013-01-01 7:30	UR	5.3	2.26	19	39.4	408	21.9	0.246	0.423	0.560	11.9	1.6	8.3	1.0	1.4	5.2	112.90	112.79
11	2013-01-19 20:45	UR + M	162.5	8.17	2725	778.0	72578	26.6	0.230	0.471	0.529	65.0	1.6	6.1	4.6	22.9	23.3	113.54	132.81
12	2013-02-11 3:00	UR	9.0	1.78	24	390.9	4507	184.2	0.251	0.421	0.579	12.2	0.9	5.5	5.6	5.6	9.4	111.99	111.97
13	2013-02-26 16:45	UR	5.3	1.68	12	851.2	4704	408.0	0.332	0.411	0.557	5.5	0.9	2.4	2.6	12.7	12.7	113.35	113.28
14	2013-03-06 18:30	UR	10.7	2.85	47	1036.3	16638	353.0	0.203	0.423	0.592	21.0	1.2	6.6	9.6	13.2	32.6	117.24	149.93
15	2013-03-07 5:30	KO	23.8	21.84	1140	473.0	51422	45.1	0.427	0.452	0.544	5.6	1.2	6.1	25.4	34.2	53.6	122.34	150.13
16	2013-03-08 5:30	UR + KO	32.0	13.93	1099	47.3	12105	11.0	0.344	0.438	0.454	11.8	1.2	5.4	6.5	40.7	60.1	123.08	137.35
17	2013-03-24 3:30	UR + M	130.2	6.99	2163	80.5	20125	9.3	0.310	0.464	0.502	31.1	0.6	2.9	4.4	22.3	22.3	115.42	138.27
18	2013-04-27 7:45	UR	5.5	4.88	29	283.2	3335	116.9	0.169	0.364	0.505	2.6	1.0	0.6	10.5	15.3	16.1	116.09	116.17
19	2013-04-29 22:30	UR	6.5	2.73	31	53.6	596	19.4	0.293	0.471	0.587	8.9	1.0	4.5	12.8	38.8	43.8	118.33	120.79

20	2013-05-01 21:15	KO	24.0	2.44	170	12.4	702	4.1	0.482	0.493	0.582	0.0	0.0	0.0	0.0	47.3	52.3	122.98	123.22
21	2013-05-16 1:00	UR	6.5	3.83	50	115.8	2193	44.0	0.143	0.214	0.404	12.1	1.0	4.8	20.5	20.5	21.9	122.91	123.00
22	2013-05-18 7:30	UR + KO	64.5	30.99	2616	163.1	67535	25.8	0.333	0.462	0.506	34.6	4.5	11.4	3.8	38.4	39.8	122.97	150.92
23	2013-05-28 15:30	UR	2.3	2.87	13	73.3	629	47.9	0.258	0.350	0.561	2.6	1.0	1.0	5.3	5.3	78.3	122.94	122.92
24	2013-09-08 4:45	UR	11.3	8.96	80	645.5	13469	167.6	0.110	0.238	0.688	38.5	12.1	37.2	3.8	3.8	3.8	112.78	114.03
25	2013-09-15 2:45	UR	14.3	6.24	44	171.8	2862	65.8	0.131	0.277	0.610	15.5	2.5	8.6	1.8	43.9	44.1	112.21	112.21
26	2013-09-29 11:45	UR	8.8	26.53	84	343.6	17274	206.0	0.069	0.346	0.551	16.1	6.3	9.5	1.8	2.4	2.4	110.54	110.80
27	2013-10-04 22:15	UR	5.3	12.83	50	199.3	5628	112.9	0.081	0.227	0.626	26.0	7.2	0.6	0.2	18.3	18.9	110.88	111.17
28	2013-10-14 15:15	UR	9.3	2.80	17	186.0	764	45.9	0.184	0.377	0.652	2.0	1.0	0.2	0.0	3.0	31.6	111.95	112.15
29	2013-12-19 15:30	UR	22.2	10.01	280	183.6	11015	39.3	0.116	0.285	0.582	81.7	2.3	9.3	4.2	4.8	5.8	115.80	149.90
30	2013-12-20 14:45	KO	29.3	26.68	1269	707.6	50102	39.5	0.340	0.420	0.525	0.0	0.0	0.6	83.5	86.5	87.3	123.22	149.97
31	2014-01-13 16:30	UR + KO	9.25	3.20	44	64.6	1319	30.2	0.217	0.362	0.504	12.7	0.8	5.3	1.8	1.8	10.8	123.00	122.60
32	2014-01-16 4:45	UR + KO	51.5	24.73	2560	81.7	45408	17.7	0.235	0.367	0.487	40.3	1.1	6.1	0.0	14.5	22.5	123.02	149.57
33	2014-01-18 14:00	UR + KO	94.0	32.78	5537	83.3	100890	18.2	0.270	0.379	0.403	37.1	2.1	5.5	26.5	77.1	79.1	123.11	150.76
34	2014-01-30 4:30	UR + KO	61.5	25.96	2781	19.2	24159	8.7	0.322	0.406	0.469	40.9	1.3	5.4	17.4	21.2	120.9	123.03	149.93
35	2014-02-05 8:00	UR + KO	51	37.54	3274	163.7	94210	28.8	0.283	0.403	0.449	29.9	1.8	6.7	4.8	73.2	79.4	123.08	151.59

Table 4: Pearson correlation matrix with significant correlation ($p<0.05$) underscored and very significant correlation ($p<0.01$) in bold for the selected flood events (n=35).

	Duration	Q_{MAX}	W_{TOT}	SSC_{MAX}	SOL_{TOT}	SSC_{AVE}	EC_{MIN}	EC_{AVE}	EC_{MAX}	TotRain	MaxInt6min	MaxInt1h	AnteRain1	AnteRain7	AnteRain14	H_{RES}
Duration																
Q_{MAX}	0.415															
W_{TOT}	**0.796**	**0.743**														
SSC_{MAX}	0.194	0.040	0.000													
SOL_{TOT}	**0.723**	**0.779**	**0.864**	0.349												
SSC_{AVE}	-0.370	-0.182	-0.384	**0.582**	-0.226											
EC_{MIN}	0.233	0.079	0.328	-0.146	0.173	-0.320										
EC_{AVE}	**0.451**	0.068	0.353	0.106	0.312	-0.261	**0.784**									
EC_{MAX}	-0.357	-0.419	**-0.530**	0.213	-0.398	0.286	-0.272	-0.180								
TotRain	**0.591**	0.391	**0.492**	0.237	**0.550**	-0.107	-0.282	-0.126	-0.059							
MaxInt6min	-0.088	0.231	-0.054	0.144	0.060	0.255	**-0.497**	**-0.505**	0.406	0.356						
MaxInt1h	-0.002	0.217	0.050	0.194	0.149	0.229	-0.355	-0.412	0.279	**0.461**	**0.802**					
AnteRain1	-0.010	0.234	0.134	0.118	0.146	-0.152	0.334	0.177	-0.267	-0.256	-0.220	-0.207				
AnteRain7	0.162	0.362	0.379	-0.162	0.304	-0.334	**0.496**	0.281	**-0.430**	-0.210	-0.259	-0.265	**0.622**			
AnteRain14	0.060	0.251	0.283	-0.295	0.095	-0.381	**0.439**	0.226	-0.346	-0.287	-0.387	-0.374	**0.451**	**0.655**		
H_{RES}	0.299	0.286	**0.492**	-0.063	0.418	**-0.461**	**0.603**	0.428	**-0.480**	0.028	-0.368	-0.251	0.236	0.361	0.385	
H_{RAGAS}	**0.569**	**0.602**	**0.734**	0.162	**0.699**	-0.316	**0.464**	**0.433**	**-0.479**	0.429	-0.248	-0.068	0.298	0.373	0.328	**0.745**

5. Discussion

Small rivers and urban streams play a decisive role on the total solid yield to the marine system. Our measurements show that a large proportion of the annual solid yield is due to flood events, but the relationship between the solid discharge and the water discharge is intricate. Investigations on main environmental parameters such as EC provide insights on the floodwater source. This section discusses the key factors of Karst Mediterranean rivers that contribute to the solid yield.

5.1. Mediterranean rivers: rainfall-discharge relationship

Overall, our data shows a typical Mediterranean river with very low water discharge at the basic low-flow level and high peaks during flood events. While our dataset covers a relatively short period of 17 months, our results seem representative and are typical of Mediterranean rivers (e.g. Rovira *et al.* 2005, Bourrin *et al.* 2008, De Girolamo *et al.* 2015). Discharge variability is similar to wadi rivers (dryland streams also called oueds), often located in semi-arid climates, where rainfall events might be highly variable both spatially and temporally (Cudennec *et al.* 2007). Such variable feature triggers runoff flood, but in a dual urban and karst environment like the Las River, largest rainfalls not always produce largest flood. The alternating low flow/flood hydrological regime of the Las River is amplified by the karst, with peculiar flood characteristics.

The hydraulic responses of both karst springs (draining the additional karst recharge area, and with typical karst fast and slow groundwater flows) and the urban watershed (runoff of the city of Toulon) enhance the highly variable discharge. When the Dardennes karst aquifer and the reservoir levels are low (e.g. during summer and autumn), the karst floods are mitigated by natural storage in the saturated and unsaturated zones of the aquifer (Baudement *et al.* 2017) and by artificial storage in the reservoir. Mediterranean karst aquifers naturally mitigate the first rainfall events during summer and autumn, e.g. in Fontaine de Vaucluse spring (catchment area 1100 km², Fleury *et al.* (2007b)), Lez spring (catchment area 130 km², Fleury *et al.*(2009), Jourde *et al.(2014)*), or Port-Miou (catchment area 400 km², Arfib and Charlier (2016)). 50 mm to more than 100 mm of cumulated rainfall is then needed in autumn to recharge those karst aquifers and activate fast groundwater flow generating springs floods. The cumulated rainfall threshold is usually assessed based on the soil and epikarst storage capacity, the non saturated zone storage and the water-table height increase. When the karst aquifer is depleted, the regulated karst water storage in the Dardennes reservoir then favors the observation of UR floods in the Las River. By contrast, during high-water periods, the very dynamic response of the aquifer to Mediterranean rainfall events generates karst floods in the river. Once the karst aquifer has been recharged in autumn, the groundwater becomes the main source of floodwater (KO), with floods lasting for days or weeks after the rainfall event. In the Dardennes case study, the dam forces the water-level to rise above the spillway, which enhances the groundwater level variation. This behaviour is yet typical of vauclusian karst aquifer and would be also observed at the Dardennes springs in natural conditions since several springs discharge at different levels, with the highest, the Ragas spring, overflowing 60 meters above the valley. The regulated karst water storage in the Dardennes Reservoir is a specific characteristic of the Las River directly impacting its discharge, but the effect of karst on floods is not unique and other case study showed that mitigation can be low (Sezen *et al.* 2019, Watlet *et al.* 2020). The highly variable discharge implies that a specific knowledge of Mediterranean rivers yield is required to better understand the coastal marine environment and develop management tools. Flood events largely contribute to annual yields of the Las River, and our assessment of the solid and liquid discharges is therefore crucial for hydro-sedimentary modeling of the Bay of Toulon (Dufresne *et al.* 2018).

5.2. Exploring the relationship between water discharge and solid discharge

The relationship between water discharge and suspended solid concentration is intricate, although the latter increases during flood events. Our results suggest the influence of water discharge on the total solid discharge, with a positive and very significant correlation between Sol_{TOT} and discharge characteristics (W_{TOT}, Q_{MAX}). However, no clear relation between *SSC* and *Q* is established for the Las River, as the maximum *SSC* and the maximum water flow peaks mismatch. This lack of relation is yet not surprising since the link between sediment load and water discharge in fluvial environments is often weak and difficult to assess (i.e. Tournoud *et al.* 2003, Regüés & Nadal-Romero 2013, Tesi *et al.* 2013, Aich *et al.* 2014).

The Mediterranean climate and the Las River catchment might explain this lack of *Q*/*SSC* relationship. Long dry periods favor sediments retention within the catchment and limit the solid discharge, enhancing the solid load during next flood events. In the Las River, the most loaded events (with highest SSC_{AVE}) often

occur following a dry period, as highlighted by the significant negative correlation between SSC_{AVE} and *AnteRain14* (Table 4): little rainfall over the 14-days previous period increases the SSC_{AVE} of a flood event. Likewise, decreasing SSC_{AVE} for several successive events demonstrates the reduction of sediments availability (Table 3, e.g. floods #3-4, 14-16). Previous floods have then probably flushed the sediment stock from the watershed, the streambed or the karst. A phenomenon of sediment exhaustion might explain the solid load variability, as the period of the year influences the suspended solid carried within a flood in Mediterranean rivers (Rovira & Batalla 2006). Characteristics of the Las River dual catchment also conceal such relationship between water discharge and solid discharge. A single empirical rating curve between *SSC* and *Q* could hence rarely be defined for Mediterranean rivers.

5.3. Contribution of floodwater sources on solid yield

The positive and very significant correlations between water levels (H_{RAGAS} and H_{RES}) and W_{TOT} clearly show the influence of the karst water in the Las River (Table 4).The EC data also corroborates the karst water inflows to the river. The positive correlations of EC_{MIN} with the levels H_{RAGAS} and H_{RES} and with previous rainfall events (*AnteRain1*, *AnteRain7*, *AnteRain14*) capable of filling the karst aquifer confirm the karst contribution to the river's discharge. The highest the levels are, the highest the EC_{MIN}. Likely, the direct input of rainwater by urban runoff during intense rainfall (high *MaxInt6*, *MaxInt1h*) induces lower EC_{MIN} (negative correlation): the more intense the rainfall is, the lower the EC_{MIN}. Low EC_{MIN} globally characterizes UR events while karst water increases EC_{MIN} (Fig. 6). The significant and positive correlation between EC_{MAX} and *MaxInt6* is yet more intricate, and its interpretation should be handled with care. Because the maximal EC is usually observed at the beginning of the flood, EC_{MAX} might actually depicts the water flowing in the river before the event. Maximal values are then observed for high proportions of water from the Saint-Antoine spring, especially at low flow. EC data distinguishes the sources of water as karst springs largely contribute to the W_{TOT} discharged to the sea.

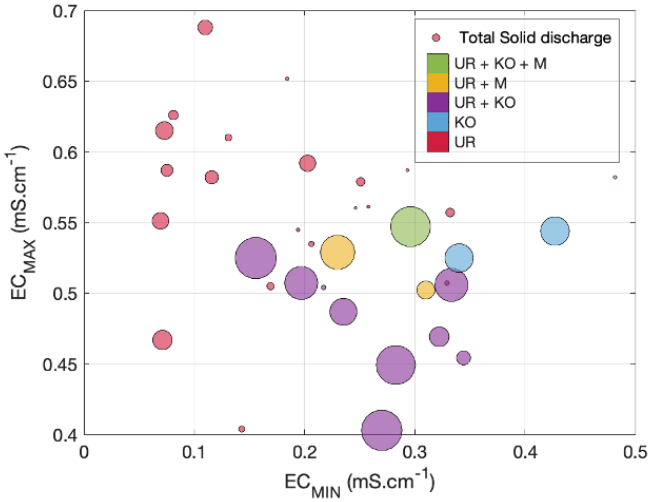

Fig. 6: Maximum electric conductivity (EC_{MAX}, $mS.cm^{-1}$) against minimum electric conductivity (EC_{MIN}, $mS.cm^{-1}$) for each flood event with size depending on total solid discharge (kg) and colorscale representing the source of water as Urban Runoff (UR), Karst Overflow (KO) and Management of the dam (M).

By impacting the liquid discharge, the source of water also influences the solid yield. The relationships between *duration*, *TotRain*, W_{TOT} and Sol_{TOT} suggest that largest rainfall events lead to longest floods and to largest water and solid discharges. Those very significant correlations (Table 4) yet conceal the relative importance of the karst on the solid discharge. The very significant and positive correlations between H_{RAGAS}, H_{RES}, W_{TOT} and Sol_{TOT} reveal that largest events receive contributions of Dardennes springs and that karst floods generate highest total solid discharge. Conversely, urban runoff floods are not responsible for biggest solid yields despite their higher SSC_{AVE} (Fig. 7). While highest EC_{MAX} values characterize UR events (Fig. 6), the negative and significant correlation between EC_{MAX} and Sol_{TOT} (Table 4) suggests that UR floods generate minimum solid yield. While one may suppose that highly intense rainfall events would increase the solid load like for other Mediterranean catchments (i.e. Nadal-Romero *et al.* 2008, Estrany *et al.* 2009), no correlation links the rainfall intensities (*MaxInt6min*, *MaxInt1h*) and solid discharge characteristics (SSC_{AVE}, SSC_{MAX}, Sol_{TOT}). SSC_{MAX} cannot be attributed to one or the other source of water

since both karst and runoff events give a wide range of values (large dots in Fig. 7). UR events thus present more loaded floods (highest SSC_{AVE}), but their shorter durations induce lower W_{TOT} and Sol_{TOT} than karst floods.

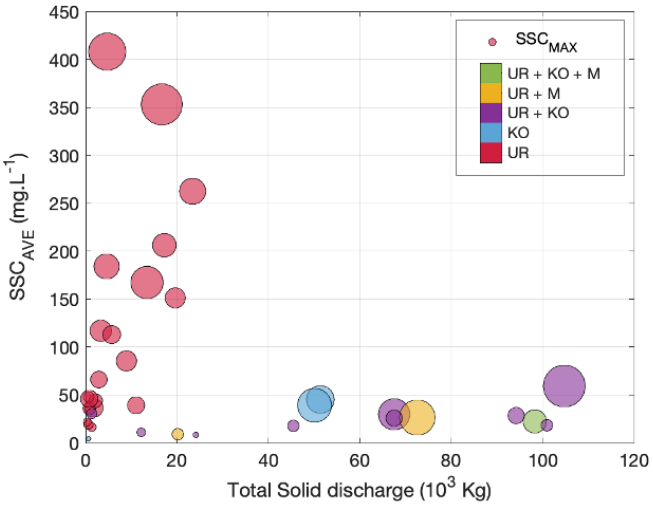

Fig. 7 Average SSC ($mg.L^{-1}$) against the total solid discharge (10^3kg) for each flood event. with size depending on SSC_{MAX} and colorscale representing the source of water as Urban Runoff (UR), Karst Overflow (KO) and Management of the dam (M).

The capacity of karst flood to yield a large amount of suspended solid relies on the regulation of the water discharge from karst springs throughout the year. Karst aquifers might store a part of the rainfall water and delay its discharge from several days, with a characteristic time-lag different for each case-study. Although we did not explore this property in this paper, the solid discharge from karst flood might also be expanded by supplementary sources of sediments from the streambed and the karst aquifer itself. The sediment storage and yield in karst watersheds are poorly documented but act as a potential sediment source to the sea that must be further investigated. Karst flood may yield a substantial amount of solid discharge, and the complex geomorphology and the extreme heterogeneity of karst systems require an interdisciplinary approach (Bonacci *et al.* 2006). In such a complex karst system exposed to flash flood and under dam regulation, the solid discharge is likely to play a decisive role in the erosion and coastline evolution (Bergillos *et al.* 2016).

5.4. Particles size variation

As small particles exhibit the capacity to transport contaminants, the grain-size of the suspended matter affects the capacity of a river to discharge contamination to the coastal ocean. Cohesive sediments (with mean diameter <63µm) form 90% of the solid yield of the Las River, which implies a considerable contamination pathway. Because of the extended deployment duration of the sediment sampler regarding floods duration (weeks *vs* hours or days), a critical analysis of samplings and water sources is intricate due to the combination of several environmental factors. Some parameters may still provide insights, such as the water levels in karst springs.

Karst flood events seem to yield coarser sediment, with an increased sand proportion in samples from the wet season (e.g. March, November, December). The positive and significant correlation between H_{RAGAS} and Q_{MAX} may imply a larger sand proportion in the samples, as higher Q_{MAX} would increase the water's ability to reach the motion threshold for coarser sediments. Samplings with the highest sand proportions also had a common characteristic, as shown in Fig. 3a,b: they all include floods following a long period of low-flow, able to flush sand sediment settled in the Las Valley or the catchment. One abundant source of sand sediment might also be upstream in the Dardennes Reservoir, fed by runoff over the limestone quarry located uphill.

Some results regarding grain-size over the November-December 2012 and February 2013 periods should yet be interpreted with caution. Roadwork in the city of Toulon created disturbed discharges and induced very turbid water at the monitoring station (Fig. 3). Those events likely increased the amount of sediment trapped by the sampler and results are non-characteristic of the Las River's normal behavior.

Uncertainties due to measurements by grain-size analyzer may also lead to an underestimation of the sand proportion. With a maximum allowed size of 2000 µm, the grain-size analyzer could not detect coarser particles. The sampler's inlet diameter (4mm) constrains the size of the trapped suspended solids, and our study might underestimate the proportion of coarser particles. Coarser sediments are more likely to be bedload transported and might present a significant proportion of the solid yield for large flood events in streams (Vericat & Batalla 2010). Bottom vertical sediment traps would then allow to assess the transport by rolling, sliding, or saltation (hopping). Otherwise, an *in situ* grain-size analyzer might improve the characterization of the suspended particles discharged by coastal rivers. Using such an analyzer would, however, imply arduous maintenance to avoid measuring drift, not to mention the risk of impacts due to large debris and thief/vandalism risks in urbanized areas and should thus be considered only for safe monitoring station.

Proportions of grain-size classes may not only exhibit events variability but may also evolve within a single flood event. A possible suspended solid concentration gradient between the surface and the bottom might also lead to an underestimation of the total solid yield. For instance, sand proportion increases within a single flood event in the Rhone River, most likely due to the water discharge, the rain intensity and the sediment availability on the watershed (Antonelli *et al.* 2008). The evolution of the sediment grain size proportion within a flood event is out of the scope of this paper, but we foster future work to focus on sediment load variability at the event's scale. Particle size variability might introduce errors in the *SSC* estimation due to its influences on the turbidity/SSC relationship, especially if grain-size varies within a flood (Lenzi & Marchi 2000, Regüés & Nadal-Romero 2013). Despite our similar relationships for low flow and floods events (see Appendix B), we believe that the influence of grain-size variations on turbidity data needs to be further explored.

5.5. Other sources of solid yield

Despite a large amount of total solid discharge by rivers to the coastal ocean, the particulate matter might end up in the marine system through other processes, such as through the air-sea interface. For instance, the annual atmospheric particulate matter deposition might reach 0.2 $g \cdot m^{-2}$ in the French Alps, 1 $g \cdot m^{-2}$ in Central France and 12 $g \cdot m^{-2}$ in Corsica (Goudie & Middleton 2001). Although seldom, exceptional Saharan dust event might induce considerable mud deposits, as one reported by Masson *et al.* (2010) in February 2002 when 13 $g \cdot m^{-2}$ deposited around the city of Toulon. By assuming a homogeneous deposit over the Little Bay (9.5 km^2), this event possibly led to a solid yield of 123.5 tons of mud. This amount is more than our biggest total solid yield for one single flood (8^{th} event, 27-30 November 2012) and represents about 15% to 20% of the annual solid discharge (710 $tons \cdot y^{-1}$ +-110) from the Las River. Atmospheric mud deposition might reach the same order of magnitude than the annual solid yield from rivers to the Western Mediterranean (Martin *et al.* 1989) and therefore might act as a major process in the sedimentary budget of the ocean, or at least, of the Western Mediterranean Sea.

6. Conclusion

This study assessed the suspended solid yield of a coastal Mediterranean river and its proportion due to flood events. With an alternating low-flow/flood regime, the Las River provides 69% of solid discharge in 11% of the time, which supports the hypothesis that floods events in coastal Mediterranean rivers largely contribute to the total solid yield. Characterization of flood events allowed the identification of environmental parameters generating large solid discharge. Mostly composed of mud (90%), the solid yield depends on the total rainfall and the total water discharge but is also highly related to the groundwater contribution of karst springs. Comparatively to karst flood, runoff induced higher suspended load (average SSC) but generated a lower total solid yield.

As our results regarding the solid discharge based on *in situ* data seems reliable, they also highlight the necessity of on-site specific calibration of the turbidity probe. Often laborious, challenging and expensive, fieldwork and measurements may, however, become easier by using simple conductivity probes. Electric conductivity data may accurately describe the floodwater source and provide valuable insights on solid discharges and sediment transport processes. Karst regions are of substantial interest since they contribute to a considerable amount of drinking water supply across Europe, and they regulate the water discharge of karst springs throughout the year. Conclusions of the present study may, therefore, be extended to several other karst Mediterranean watersheds, with decisive consequences on the sediment yield for estuarine systems and coastal marine environment.

7. Acknowledgements

The authors wish to thank T.Lamarque and SpéléH2O for his involvement in measurements for the rating curve and Toulon Provence Méditerranée (TPM) for its founding. Ch.D. is grateful to IRSN and Region PACA for the funding of this research. We thank *Météo-France* for the meteorological data. This work benefited from the fruitful discussions within the framework of the KARST observatory network (www.sokarst.org) initiative from the INSU/CNRS, which aims to strengthen knowledge sharing and promote cross-disciplinary research on karst systems. Dardennes springs data have been monitored in the frame of the DARDENNES project funded by the Agence de l'Eau (RMC), the city of Toulon, Veolia Eau, Cenote Company, and Aix-Marseille University. The authors also wish to thank all persons who participated in the fieldwork. We are very grateful to the anonymous reviewers for the valuable criticisms, which substantially improved the quality of the manuscript.

8. References

Aich, V., A. Zimmermann and H. Elsenbeer (2014). "Quantification and interpretation of suspended-sediment discharge hysteresis patterns: How much data do we need?" CATENA **122**: 120-129.

Alexandrov, Y., J. B. Laronne and I. Reid (2003). "Suspended sediment concentration and its variation with water discharge in a dryland ephemeral channel, northern Negev, Israel." Journal of Arid Environments **53**(1): 73-84.

Alexandrov, Y., J. B. Laronne and I. Reid (2007). "Intra-event and inter-seasonal behaviour of suspended sediment in flash floods of the semi-arid northern Negev, Israel." Geomorphology **85**(1–2): 85-97.

Antonelli, C., F. Eyrolle, B. Rolland, M. Provansal and F. Sabatier (2008). "Suspended sediment and 137Cs fluxes during the exceptional December 2003 flood in the Rhone River, southeast France." Geomorphology **95**(3–4): 350-360.

Arfib, B. and J.-B. Charlier (2016). "Insights into saline intrusion and freshwater resources in coastal karstic aquifers using a lumped Rainfall–Discharge–Salinity model (the Port-Miou brackish spring, SE France)." Journal of Hydrology **540**: 148-161.

Baudement, C., B. Arfib, N. Mazzilli, J. Jouves, T. Lamarque and Y. Guglielmi (2017). "Groundwater management of a highly dynamic karst by assessing baseflow and quickflow with a rainfall-discharge model (Dardennes springs, SE France)." Bull. Soc. géol. Fr. **188**(6): 40.

Bergillos, R. J., C. Rodríguez-Delgado, A. Millares, M. Ortega-Sánchez and M. A. Losada (2016). "Impact of river regulation on a Mediterranean delta: Assessment of managed versus unmanaged scenarios." Water Resources Research **52**(7): 5132-5148.

Bezak, N., M. Brilly and M. Šraj (2014). "Comparison between the peaks-over-threshold method and the annual maximum method for flood frequency analysis." Hydrological Sciences Journal **59**(5): 959-977.

Bonacci, O., I. Ljubenkov and T. Roje-Bonacci (2006). "Karst flash floods: an example from the Dinaric karst (Croatia)." Natural Hazards and Earth System Science **6**(2): 195-203.

Bourrin, F., P. L. Friend, C. L. Amos, E. Manca, C. Ulses, A. Palanques, X. Durrieu de Madron and C. E. L. Thompson (2008). "Sediment dispersal from a typical Mediterranean flood: The Têt River, Gulf of Lions." Continental Shelf Research **28**(15): 1895-1910.

Capello, M., L. Cutroneo, G. Ferretti, S. Gallino and G. Canepa (2016). "Changes in the physical characteristics of the water column at the mouth of a torrent during an extreme rainfall event." Journal of Hydrology **541**: 146-157.

Chen, Z., A. S. Auler, M. Bakalowicz, D. Drew, F. Griger, J. Hartmann, G. Jiang, N. Moosdorf, A. Richts and Z. Stevanovic (2017). "The World Karst Aquifer Mapping project: concept, mapping procedure and map of Europe." Hydrogeology Journal **25**(3): 771-785.

Chow, V. T. (2010). Applied hydrology, Tata McGraw-Hill Education.

Claps, P. and F. Laio (2003). "Can continuous streamflow data support flood frequency analysis? An alternative to the partial duration series approach." Water Resources Research **39**(8).

Cudennec, C., C. Leduc and D. Koutsoyiannis (2007). "Dryland hydrology in Mediterranean regions—a review." Hydrological Sciences Journal **52**(6): 1077-1087.

Dang, D. H., V. Lenoble, G. Durrieu, D. Omanovic, J. U. Mullot, S. Mounier and C. Garnier (2015). "Seasonal variations of coastal sedimentary trace metals cycling: Insight on the effect of manganese and iron (oxy)hydroxides, sulphide and organic matter." Mar Pollut Bull **92**(1-2): 113-124.

Dang, D. H., E. Tessier, V. Lenoble, G. Durrieu, D. Omanović, J.-U. Mullot, H.-R. Pfeifer, S. Mounier and C. Garnier (2014). "Key parameters controlling arsenic dynamics in coastal sediments: An analytical and modeling approach." Marine Chemistry **161**: 34-46.

De Girolamo, A. M., G. Pappagallo and A. Lo Porto (2015). "Temporal variability of suspended sediment transport and rating curves in a Mediterranean river basin: The Celone (SE Italy)." CATENA **128**: 135-143.

Dufresne, C., C. Duffa, V. Rey and R. Verney (2018). "Hydro-sedimentary model as a post-accidental management tool: Application to radionuclide marine dispersion in the Bay of Toulon (France)." Ocean & Coastal Management **153**: 176-192.

Estrany, J., C. Garcia and R. J. Batalla (2009). "Suspended sediment transport in a small Mediterranean agricultural catchment." Earth Surface Processes and Landforms **34**(7): 929-940.

Fleury, P., M. Bakalowicz and G. de Marsily (2007a). "Submarine springs and coastal karst aquifers: a review." Journal of Hydrology **339**(1-2): 79-92.

Fleury, P., B. Ladouche, Y. Conroux, H. Jourde and N. Dörfliger (2009). "Modelling the hydrologic functions of a karst aquifer under active water management–the Lez spring." Journal of Hydrology **365**(3-4): 235-243.

Fleury, P., J.-C. Maréchal and B. Ladouche (2013). "Karst flash-flood forecasting in the city of Nîmes (southern France)." Engineering Geology **164**: 26-35.

Fleury, P., V. Plagnes and M. Bakalowicz (2007b). "Modelling of the functioning of karst aquifers with a reservoir model: Application to Fontaine de Vaucluse (South of France)." Journal of hydrology **345**(1-2): 38-49.

Gaume, E., V. Bain, P. Bernardara, O. Newinger, M. Barbuc, A. Bateman, L. Blaškovičová, G. Blöschl, M. Borga and A. Dumitrescu (2009). "A compilation of data on European flash floods." Journal of Hydrology **367**(1-2): 70-78.

Goudie, A. S. and N. J. Middleton (2001). "Saharan dust storms: nature and consequences." Earth-Science Reviews **56**(1–4): 179-204.

Jourde, H., A. Lafare, N. Mazzilli, G. Belaud, L. Neppel, N. Dörfliger and F. Cernesson (2014). "Flash flood mitigation as a positive consequence of anthropogenic forcing on the groundwater resource in a karst catchment." Environmental earth sciences **71**(2): 573-583.

Jouves, J., S. Viseur, B. Arfib, C. Baudement, H. Camus, P. Collon and Y. Guglielmi (2017). "Speleogenesis, geometry, and topology of caves: A quantitative study of 3D karst conduits." Geomorphology **298**: 86-106.

Jungerius, P. D. and M. J. ten Harkel (1994). "The effect of rainfall intensity on surface runoff and sediment yield in the grey dunes along the Dutch coast under conditions of limited rainfall acceptance." CATENA **23**(3–4): 269-279.

Lamarque, T. (2014). Etablissement d'une courbe de tarage des débits du cours d'eau du Las, Spélé-H20**:** 103 (in french).

Lang, M., T. Ouarda and B. Bobée (1999). "Towards operational guidelines for over-threshold modeling." Journal of hydrology **225**(3-4): 103-117.

Lenzi, M. A. and L. Marchi (2000). "Suspended sediment load during floods in a small stream of the Dolomites (northeastern Italy)." CATENA **39**(4): 267-282.

López-Tarazón, J. A., R. J. Batalla, D. Vericat and J. C. Balasch (2010). "Rainfall, runoff and sediment transport relations in a mesoscale mountainous catchment: The River Isábena (Ebro basin)." CATENA **82**(1): 23-34.

López-Tarazón, J. A., R. J. Batalla, D. Vericat and T. Francke (2012). "The sediment budget of a highly dynamic mesoscale catchment: The River Isábena." Geomorphology **138**(1): 15-28.

Martin, J.-M., F. Elbaz-Poulichet, C. Guieu, M.-D. Loÿe-Pilot and G. Han (1989). "River versus atmospheric input of material to the mediterranean sea: an overview." Marine Chemistry **28**(1–3): 159-182.

Masson, O., D. Piga, R. Gurriaran and D. D'Amico (2010). "Impact of an exceptional Saharan dust outbreak in France: PM10 and artificial radionuclides concentrations in air and in dust deposit." Atmospheric Environment **44**(20): 2478-2486.

Meriano, M., K. W. Howard and N. Eyles (2011). "The role of midsummer urban aquifer recharge in stormflow generation using isotopic and chemical hydrograph separation techniques." Journal of hydrology **396**(1-2): 82-93.

Meybeck, M., L. Laroche, H. H. Durr and J. P. M. Syvitski (2003). "Global variability of daily total suspended solids and their fluxes in rivers." Global and Planetary Change **39**(1-2): 65-93.

Moraetis, D., D. Efstathiou, F. Stamati, O. Tzoraki, N. P. Nikolaidis, J. L. Schnoor and K. Vozinakis (2010). "High-frequency monitoring for the identification of hydrological and bio-geochemical processes in a Mediterranean river basin." Journal of Hydrology **389**(1): 127-136.

Nadal-Romero, E., D. Regüés and J. Latron (2008). "Relationships among rainfall, runoff, and suspended sediment in a small catchment with badlands." CATENA **74**(2): 127-136.

Nicolau, R., Y. Lucas, P. Merdy and M. Raynaud (2012). "Base flow and stormwater net fluxes of carbon and trace metals to the Mediterranean sea by an urbanized small river." Water Research **46**(20): 6625-6637.

Pellerin, B. A., W. M. Wollheim, X. Feng and C. J. Vörösmarty (2008). "The application of electrical conductivity as a tracer for hydrograph separation in urban catchments." Hydrological Processes: An International Journal **22**(12): 1810-1818.

Perrin, J.-L. and M.-G. Tournoud (2009). "Hydrological processes controlling flow generation in a small Mediterranean catchment under karstic influence." Hydrological Sciences Journal **54**(6): 1125-1140.

Pfannkuche, J. and A. Schmidt (2003). "Determination of suspended particulate matter concentration from turbidity measurements: particle size effects and calibration procedures." Hydrological Processes **17**(10): 1951-1963.

Phillips, J. M., M. A. Russell and D. E. Walling (2000). "Time-integrated sampling of fluvial suspended sediment: a simple methodology for small catchments." Hydrological Processes **14**(14): 2589-2602.

Pilgrim, D. H., D. D. Huff and T. D. Steele (1979). "Use of specific conductance and contact time relations for separating flow components in storm runoff." Water Resources Research **15**(2): 329-339.

Regüés, D. and E. Nadal-Romero (2013). "Uncertainty in the evaluation of sediment yield from badland areas: Suspended sediment transport estimated in the Araguás catchment (central Spanish Pyrenees)." CATENA **106**(0): 93-100.

Robson, A., C. Neal, C. J. Smith and S. Hill (1992). "Short-term variations in rain and stream water conductivity at a forested site in mid-Wales — implications for water movement." Science of The Total Environment **119**(0): 1-18.

Robson, A. J., C. Neal, S. Hill and C. J. Smith (1993). "Linking variations in short- and medium-term stream chemistry to rainfall inputs — some observations at Plynlimon, Mid-Wales." Journal of Hydrology **144**(1–4): 291-310.

Rovira, A. and R. J. Batalla (2006). "Temporal distribution of suspended sediment transport in a Mediterranean basin: The Lower Tordera (NE SPAIN)." Geomorphology **79**(1-2): 58-71.

Rovira, A., R. J. Batalla and M. Sala (2005). "Fluvial sediment budget of a Mediterranean river: the lower Tordera (Catalan Coastal Ranges, NE Spain)." CATENA **60**(1): 19-42.

Russell, M., D. Walling and R. Hodgkinson (2000). "Appraisal of a simple sampling device for collecting time-integrated fluvial suspended sediment samples." IAHS Publication(International Association of Hydrological Sciences)(263): 119-127.

Schnegg, P.-A., C. Perret, A. Hauet, D. Parrel, G. Saysset and P. Vignon (2011). Stream gauging by dilution of fluorescent tracers and state of the art of the EDF hydroclimatological observation network. Proc. 9th Conference on Limestone Hydrogeology, Besançon.

Serrat, P. (1999). "Dynamique sédimentaire actuelle d'un système fluvial méditerranéen: l'Agly (France): Present sediment yield from a Mediterranean fluvial system: the Agly river (France)." Comptes Rendus de l'Académie des Sciences - Series IIA - Earth and Planetary Science **329**(3): 189-196 (in french).

Serrat, P., W. Ludwig, B. Navarro and J.-L. Blazi (2001). "Variabilité spatio-temporelle des flux de matières en suspension d'un fleuve côtier méditerranéen : la Têt (France)." Comptes Rendus de l'Académie des Sciences - Series IIA - Earth and Planetary Science **333**(7): 389-397 (in french).

Sezen, C., N. Bezak, Y. Bai and M. Šraj (2019). "Hydrological modelling of karst catchment using lumped conceptual and data mining models." Journal of Hydrology **576**: 98-110.

Skoulikidis, N. and Y. Amaxidis (2009). "Origin and dynamics of dissolved and particulate nutrients in a minimally disturbed Mediterranean river with intermittent flow." Journal of Hydrology **373**(1): 218-229.

Skoulikidis, N. T., S. Sabater, T. Datry, M. M. Morais, A. Buffagni, G. Dörflinger, S. Zogaris, M. del Mar Sánchez-Montoya, N. Bonada and E. Kalogianni (2017). "Non-perennial Mediterranean rivers in Europe: status, pressures, and challenges for research and management." Science of the Total Environment **577**: 1-18.

Struglia, M. V., A. Mariotti and A. Filograsso (2004). "River Discharge into the Mediterranean Sea: Climatology and Aspects of the Observed Variability." Journal of Climate **17**(24): 4740-4751.

Tesi, T., S. Miserocchi, F. Acri, L. Langone, A. Boldrin, J. A. Hatten and S. Albertazzi (2013). "Flood-driven transport of sediment, particulate organic matter, and nutrients from the Po River watershed to the Mediterranean Sea." Journal of Hydrology **498**(0): 144-152.

Tessier, E., C. Garnier, J. U. Mullot, V. Lenoble, M. Arnaud, M. Raynaud and S. Mounier (2011). "Study of the spatial and historical distribution of sediment inorganic contamination in the Toulon bay (France)." Mar Pollut Bull **62**(10): 2075-2086.

Tournoud, M. G., C. Salles, B. Picot, S. Payraudeau and C. Rodier (2003). "Sediment and nutrient flood loads in three small Mediterranean catchments." IAHS PUBLICATION: 484-492.

Tzoraki, O., N. P. Nikolaidis, Y. Amaxidis and N. T. Skoulikidis (2007). "In-Stream Biogeochemical Processes of a Temporary River." Environmental Science & Technology **41**(4): 1225-1231.

Valdes, D., J.-P. Dupont, N. Massei, B. Laignel and J. Rodet (2006). "Investigation of karst hydrodynamics and organization using autocorrelations and T–ΔC curves." Journal of Hydrology **329**(3–4): 432-443.

Vericat, D. and R. J. Batalla (2010). "Sediment transport from continuous monitoring in a perennial Mediterranean stream." CATENA **82**(2): 77-86.

Watlet, A., M. Van Camp, O. Francis, A. Poulain, G. Rochez, V. Hallet, Y. Quinif and O. Kaufmann (2020). "Gravity monitoring of underground flash flood events to study their impact on groundwater recharge and the distribution of karst voids." Water Resources Research **56**(4): e2019WR026673.

Zabaleta, A., M. Martínez, J. A. Uriarte and I. Antigüedad (2007). "Factors controlling suspended sediment yield during runoff events in small headwater catchments of the Basque Country." CATENA **71**(1): 179-190.

9. Appendices

A. **Sediment sampler**

The sediment sampler has shown its efficiency to trap representative samples regarding small particles and low flow velocities (Phillips *et al.* 2000). To ensure the efficiency of the device in the Las River, Fig.A 1 shows the dry mass from collected samples and the total solid yield for the deployment period assessed with the turbidity probe. The good correlation between the sampled mass and the estimated solid discharge suggests that the device is efficient regarding solid yield. However, no data allows us to verify the representativeness of the sampler regarding grain-size.

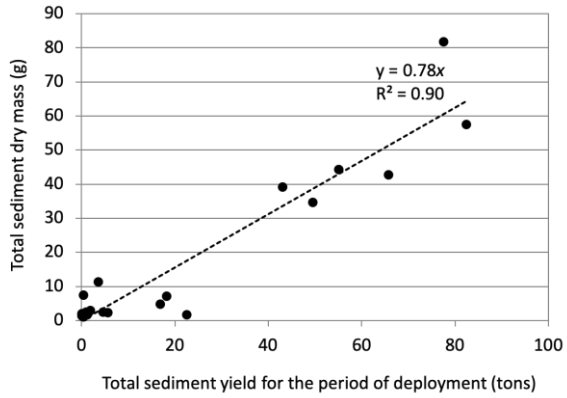

Fig.A 1. Total dry mass (g) collected by the sediment sampler in relation to the total solid discharge (tons) over the deployment period for the 29 samples

B. **Turbidity / SSC relation**

The SSC is deduced from turbidity data, which indicates the water opacity. The turbidity unit of measurement, the nephelometric turbidity unit (NTU), depends on probes sensitivity and the suspended matter characteristics. Parameters such as the size and the mineralogy of particles (Lenzi & Marchi 2000) and river's discharge (Pfannkuche & Schmidt 2003) may induce high variability of the recorded turbidity data and interfere with the estimation of the SSC. Since the suspended matter characteristics change depending on location and river, it is essential to establish a single relationship between the turbidity data and the SSC for each monitoring station. Recorded turbidity data were compared to SSC from the water samplings filtrations to define an NTU/SSC specific relationship. The turbidity dataset (NTU) is plotted against SSC ($mg \cdot L^{-1}$) from the water samplings filtrations during low flow (light blue) and flood events (dark blue) (Fig.B 1). SSC/NTU relationship for all data (n=155) is significant, with R^2=0.953. Eq.(B.1) converts turbidity data (NTU) to suspended sediment concentration (SSC).

$$SSC = 0.996 \cdot NTU \qquad \text{Eq.(B.1)}$$

SSCs from water samples show good agreement with calculated concentrations from the turbidity dataset. For the 155 couples of calculated and filtered concentrations, the root mean square error (RMSE) is 40.6 $mg \cdot L^{-1}$ with a normalized RMSE equals to 4%. When focusing on concentrations at low-flow, RMSE=3.3 $mg \cdot L^{-1}$ and NRMSE=21%. For flood events, RMSE=44.6 $mg \cdot L^{-1}$ and NRMSE=4%.

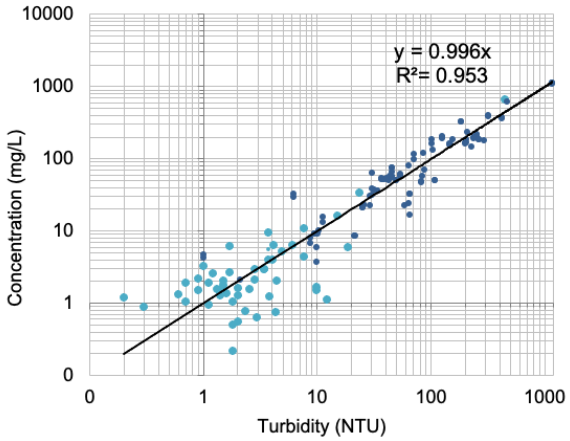

Fig.B 1. Scatter plot of the suspended solid concentration ($mg \cdot L^{-1}$) and turbidity (NTU) for low flow recorded data (light blue) and flood recorded data (dark blue). Linear regression, coefficients and R^2 are shown for all *in situ* data (black).